Abel Inversion Scheme for Marked Improvement of a Reflectron Time-of-Flight Mass Spectrometer

Kinugawa, Tohru

Furuhashi, Osamu

Abel Inversion Scheme for Marked Improvement of a Reflectron Time-of-Flight Mass Spectrometer

Tohru Kinugawa[1*], Osamu Furuhashi[2]

[1]*Institute for Promotion of Higher Education, Kobe University, Kobe 657-8501, Japan*
[2]*Technology Research Laboratory, Shimadzu Corporation, Kyoto 604-8511, Japan*

This letter describes a simple Abel inversion scheme for marked improvement of a reflectron time-of-flight (TOF) mass spectrometer having a reflecting electric potential $U(X)$ along its central axis X. To maximize the resolving power, the inverse function $X(U)$ was determined using the Abel inversion of the most-desirable TOF $\tau(E)$, which is a function of the total energy E. Based on the linear nature of the Abel transform, we could derive an additional condition necessary for the electrostatic realization of $X(U)$. Our numerical results demonstrated the definite superiority of this approach compared with the conventional energy-focusing method.

Abel's mechanical problem (AMP)[1–3] is an inverse problem of historical importance. In terms of modern mechanics,[4] AMP introduced the Abel inversion[5] to determine an unknown one-dimensional potential $U(X)$. For this inversion, the input is the temporal period $\tau(E)$ for a particle having total energy E to travel within the spatial region of $U(X)$. The entire procedure is simply the linear Abel transform of $\tau(E)$ to $X(U)$, i.e., the inverse function of $U(X)$. Following recent work,[6] we applied this inversion scheme to the common time-of-flight (TOF) mass spectrometer called a reflectron[7] to achieve a marked improvement. Our theoretical discussion emphasizes the electrostatic realization of $X(U)$ based on the linear nature of the Abel transform. We also provide numerical results demonstrating the definite superiority of this approach compared with the conventional energy-focusing method (see Fig. 4). As detailed in the Supplemental Material,[8] the present inversion scheme is of practical use for suppressing the turn-around time.

Our idea is specifically intended for a reflectron.[7] As sketched in Fig. 1(a), this spectrometer delivers a short-pulsed bunch of ions into flight and determines their mass-to-charge ratios M/q by recording and analyzing the resultant TOF spectrum. In the X direction, the

*kinugawa@phoenix.kobe-u.ac.jp

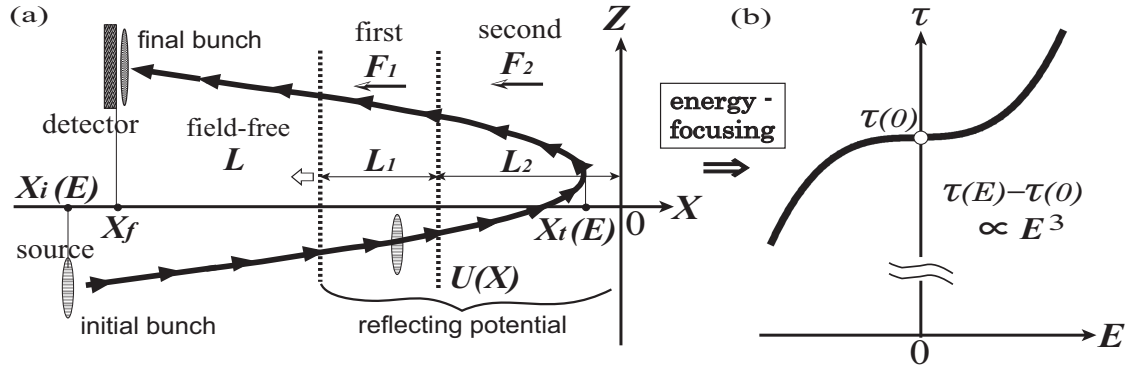

Fig. 1. Conventional reflectron mass spectrometer: (a) configuration consisting of two stages with uniform fields and, (b) TOF function $\tau(E)$ satisfying the second-order energy-focusing in (2).

ions undergo an extensive field-free flight and a short reflection by the electrostatic potential $U(X)$. Meanwhile, they maintain uniform motion in the Z direction without affecting the total TOF T. Therefore, our goal is to realize $U(X)$ that maximizes the resolving power. For this purpose, let us first recall that the speed of a charged particle is $\sqrt{2\{E-U(X)\}}/\sqrt{M/q}$ at X, because of the conservation of E, which is the sum of the potential and kinetic energies. Then, T depends on E and M/q:

$$T(E,M/q) = \left| \int_{X_i(E)}^{X_t(E)} \frac{\sqrt{M/q}\,dX}{\sqrt{2\{E-U(X)\}}} \right| + \left| \int_{X_t(E)}^{X_f} \frac{\sqrt{M/q}\,dX}{\sqrt{2\{E-U(X)\}}} \right| = \sqrt{M/q}\cdot\tau(E), \tag{1}$$

where $X_i(E)$ and X_f are the X coordinates of the initial and final positions, respectively. In addition, $X_t(E)$ represents the turning point satisfying $E = U(X_t)$ within the reflecting potential. Generally, $X_i(E)$ and $X_t(E)$ are functions of E, whereas X_f is a constant fixed at the detector's position. $\tau(E)$ is the reduced TOF of $T(E,M/q)/\sqrt{M/q}$ that depends on E alone. In this letter, we refer to the reduced form similar to $\tau(E)$ as a TOF function or simply a TOF. To maximize the resolving power of a reflectron, one should keep $\tau(E)$ as constant as possible so that T makes a perfect marker of $\sqrt{M/q}$ from (1). This constancy was achieved only in an approximate manner by the first reflectron.[7] As depicted in Fig. 1 (a), the potential $U(X)$ was produced, based on two stages with constant-field strengths of F_1 and F_2 that covered spatial lengths of $L_1$and L_2, respectively. Next, these parameters and the total length of the field-free flight L were adjusted to satisfy the second-order energy-focusing:

$$\left(\frac{d\tau}{dE}\right) = \left(\frac{d^2\tau}{dE^2}\right) = 0, \tag{2}$$

where the derivatives are evaluated at a given energy, say $E = 0$. As demonstrated in Fig. 1(b), this focusing produced

$$\tau(E) - \tau(0) \approx (1/6)\left(\frac{d^3\tau}{dE^3}\right)E^3, \tag{3}$$

and the constancy of $\tau(E)$ was approximately achieved within a narrow region of E. Similar treatments have been adopted since the invention of the reflectron.[7]

Instead of this conventional energy-focusing method, we propose a simple and strict inversion scheme[6] to satisfy the perfect isochronicity, specifically, $\tau(E \geq 0) = \tau_0 =$ constant [cf. Fig. 2 (b)]. In this scheme, the entire spectrometer is cut into two regions: the A-type in $X > 0$ and the N-type in $X < 0$, as shown in Fig. 2 (a). By definition, we have $U(X = 0) \equiv 0$. In the A-type region, we consider that the reflecting potential $U_A(X)$ and travel time $\tau_A(E)$ are unknowns to be determined later. In the N-type region, however, the potential $U_N(X)$ and travel time $\tau_N(E)$ are predetermined. To maximize the resolving power, the most-desirable TOF must be $\tau_A(E) = \tau(E) - \tau_N(E) = \tau_0 - \tau_N(E)$ because the perfect isochronicity is satisfied in reverse. From Eq.(13) in Ref. 6, we can determine $X_A(U)$, i.e., the inverse function of $U_A(X)$ using the Abel inversion of $\tau_A(E)$ with the use of the Abel operator $A = \left(1/\sqrt{\pi}\right)\int_0^U dE/\sqrt{U-E}$:

$$\begin{aligned} X_A(U) &= \frac{1}{\sqrt{2\pi}}A\left[\tau_A(E)\right] = \frac{1}{\sqrt{2\pi}}A\left[\tau_0 - \tau_N(E)\right] \\ &= \frac{\sqrt{2}\,\tau_0}{\pi}\sqrt{U} - \frac{1}{\sqrt{2\pi}}A\left[\tau_N(E)\right]. \end{aligned} \tag{4}$$

In the last expression, the contributions from $A[\tau_0]$ and $A[\tau_N(E)]$ are separated because A is linear. Thus, our scheme is as simple as determining $X_A(U)$ using the Abel inversion once $\tau_N(E)$ and $\tau(E \geq 0)$ are predetermined.

Next, we mention the most crucial factor for performing the present scheme, namely, the electrostatic realization of $X_A(U)$. Although the inversion formula in (4) demands no restriction on either the TOF function $\tau_N(E)$ or the constant τ_0, we learned a peculiar tendency in the numerical simulations. Specifically, the resultant $X_A(U)$ can be rarely created in vacuum by electrostatic means if $\tau_N(E)$ and τ_0 are freely given. Theoretically, this failure can be attributed to the essential nature of Laplace's equation: the potential $U_A(X)$ permits no singularity within the space of no electric charges as long as $U_A(X)$ satisfies Laplace's equation. In contrast, there must be some singularity at $U = 0$ if $X_A(U)$ is given by the Abel inversion scheme, as reasoned below.

To discuss this singularity of $X_A(U)$, we first note that $U_N(X < 0)$ is highly smooth, which

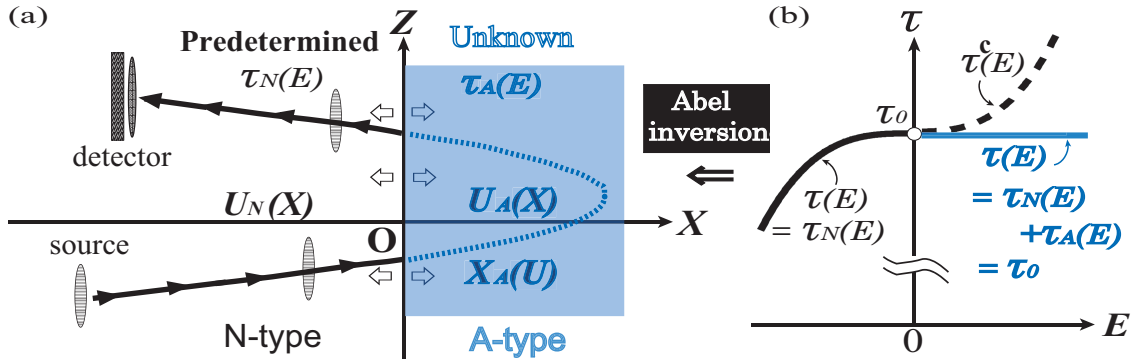

Fig. 2. (Color online) Abel inversion scheme: (a) configuration consisting of the predetermined N-type and unknown A-type regions and, (b) TOF function $\tau(E)$ satisfying $\tau(E \geq 0) = \tau_0 =$ constant. For comparison, the imaginary but conventional $\tau^{\mathbf{c}}(E)$ is also displayed as a dotted curve.

is attributed to Laplace's equation. Therefore, $U_N(X < 0)$ is smoothly extended to the A-type region in $X > 0$. For practical reflectrons, this smooth $U_N(X)$ monotonically increases near $X = U = 0$ [see Fig.3 (a)]. Therefore, we also have the inverse function $X_N(U)$ that is highly smooth near $X = 0$. Next, we imagine that this highly smooth $U_N(X)$ [equivalently $X_N(U)$] is created around $X = U = 0$. For this imaginary case that recalls conventional reflectrons, the total TOF and travel time spent in the A-type region are represented by $\tau^{\mathbf{c}}(E)$ and $\tau^{\mathbf{c}}_A(E)$, respectively. In the N-type region, we similarly denote the imaginary but conventional distributions by $U^{\mathbf{c}}_N(X > 0)$ and $X^{\mathbf{c}}_N(U > 0)$. Because these conventional potentials are highly continuous, the resultant $\tau^{\mathbf{c}}(E)$ values are usually represented by the Taylor series:

$$\tau^{\mathbf{c}}(E) = \tau^{\mathbf{c}}(0) + \tau^{\mathbf{c}(1)}(0)E + \cdots + \tau^{\mathbf{c}(n)}(0)E^n/n! + \cdots,$$

where $\tau^{\mathbf{c}(n)}(0)$ is the nth-order derivatives at $E = 0$. Concerning the total TOF, we have $\tau^{\mathbf{c}}(E) = \tau_N(E) + \tau^{\mathbf{c}}_A(E)$ and $\tau_0 = \tau_N(E) + \tau_A(E)$. Hence, the difference of these equations yields

$$\tau_A(E) - \tau^{\mathbf{c}}_A(E) = \tau_0 - \tau^{\mathbf{c}}(E)$$

$$= -\Delta\tau_0 - \tau^{\mathbf{c}(1)}(0)E - \cdots - \tau^{\mathbf{c}(n)}(0)E^n/n! - \cdots,$$

where $\Delta\tau_0 \equiv \tau^{\mathbf{c}}(0) - \tau_0$. By taking the difference of the linear Abel transforms between $X_A(U) = (1/\sqrt{2\pi})A\left[\tau_A(E)\right]$ and $X^{\mathbf{c}}_N(U) = (1/\sqrt{2\pi})A\left[\tau^{\mathbf{c}}_A(E)\right]$, we obtain

$$X_A(U) - X^{\mathbf{c}}_N(U) = \left(1/\sqrt{2\pi}\right)A\left[\tau_A(E) - \tau^{\mathbf{c}}_A(E)\right]$$

$$= -A\left[\Delta\tau_0 + \tau^{\mathbf{c}(1)}(0)E + \cdots + \tau^{\mathbf{c}(n)}(0)E^n/n! + \cdot\cdot\right] / \sqrt{2\pi},$$

performing the Abel transform in a termwise manner

$$= -\left(\sqrt{2}\Delta\tau_0/\pi\right) U^{1/2} - a_1 U^{3/2} - \cdots - a_n U^{n+1/2} - \cdot\cdot, \tag{5}$$

where $a_n = \tau^{\mathbf{c}(n)}(0)/\left[\sqrt{2\pi}\,\Gamma(n+3/2)\right]$. Thus, $X_A(U)$ must be a sum of the analytic $X_N(U)$ and a non-analytic part expanded into a half-integer series of U. Because of this non-analytic part, the higher-order derivatives of $X_A(U)$ always become singular at $X = U = 0$.

Because this singularity seemingly contradicts the extreme smoothness essential to the electrostatic realization of $U_A(x)$, one naturally doubts the feasibility of the present inversion scheme. However, our expectation is the opposite; the singularity can be neatly controlled by eliminating $\Delta\tau_0$ and a_n up to the highest possible order n. Specifically, we can set $\Delta\tau_0 = 0$ without losing generality as τ_0 is arbitrary. In addition, (5) indicates that we have $a_1 = a_2 = \cdot\cdot = a_n = 0$ when the nth-order energy focusing is satisfied:

$$\tau^{\mathbf{c}(1)}(0) = \tau^{\mathbf{c}(2)}(0) = \cdot\cdot = \tau^{\mathbf{c}(n)}(0) = 0, \tag{6}$$

which constitutes a natural extension of the second-order energy-focusing in (2). Therefore, our objective is to weaken the singularity by increasing the order n in (6). From (5) and (6), we have

$$X_A - X_N \approx -a_{n+1} U^{n+3/2}, \tag{7}$$

which is continuous up to the $(n+1)$th-order derivatives at $U = 0$, and the singularity is expectedly reduced if n is increased.

This anticipation was numerically confirmed for the example with n being as small as 2: the N-type region is identically configured to the two-staged reflectron in Fig. 1(a). Fig. 3(a) shows the potential distribution, consisting of the linear $U_N(X)$ to satisfy the second-order focusing in (2) and the weakly nonlinear $X_A(U)$ for the perfect isochronicity of $\tau(E \geq 0) = \tau(0)$. Specifically, we set $F_1 = 127.1110$ V/mm, $F_2 = 13.50825$ V/mm, $L_1 = 30$ mm, $L_2 = 132.2654$ mm and the length of the field-free flight $L = 1400$ mm while the width of the source was neglected for simplicity. This setting offers the highest feasibility because the N-type region is nearly identical to conventional reflectrons. For this example, another merit is that $X_A(U)$ can be described in an analytic form (see Section IV in Ref.6) such that the ambiguities in numerical treatments are minimized. Our computations started with the analytic $X_A(U)$ and proceeded to numerical simulations aimed at the electrostatic realization of $U_A(X)$ by placing electrodes at regular intervals in vacuum. Specifically, we employed

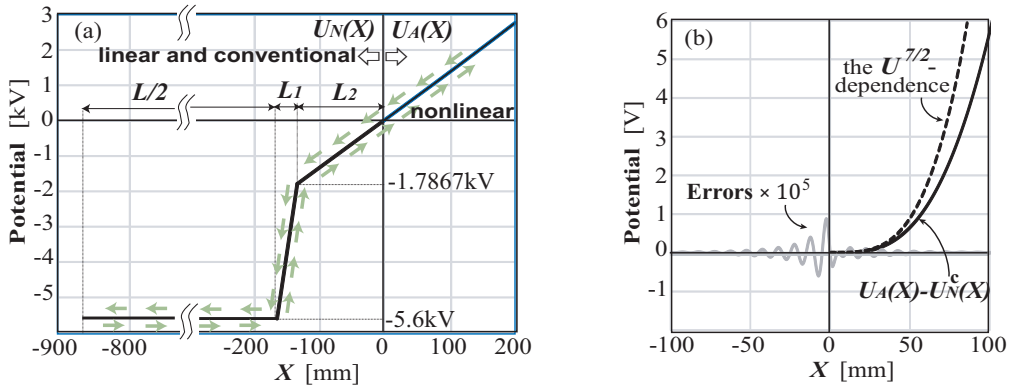

Fig. 3. (Color online) Potential distributions simulated for the example detailed in the text. (a) $U_A(X)$ and $U_N(X)$. (b) $U_A(X) - U_N^c(X)$ [black solid] and the $U^{7/2}$-dependence expected from (7) [dashed]. The errors of the spline-based $U_A(X)$ [gray solid] are expanded by a factor of 10^5.

the spline interpolation[9] of $U_A(X)$ at 5-mm intervals, which is continuous up to the 22nd-order derivatives and provides sufficient smoothness to imitate the potential in vacuum. As observed in Fig. 3(a), this spline-based $U_A(X)$ is smoothly connected to $U_N(X)$ at $X = 0$. Fig. 3(b) presents $U_A(X) - U_N^c(X)$. Although the graph is significantly enlarged, the singularity remains indiscernible but well-explained by the $U^{7/2}$-dependence expected from (7). In the same figure, the errors of the spline-based $U_A(X)$ are observed to be less than 8×10^{-6} V. In Fig. 4, the dimensionless TOF function $\Delta\tilde{\tau} \equiv [\tau(E) - \tau(0)]\,/\tau(0)$ computed using this spline-based $U_A(X)$ exhibits excellent constancy; the deviations from the predetermined values are less than 7×10^{-9}. For comparison, Fig. 4 also presents $\Delta\tilde{\tau}^{\mathbf{c}} \equiv [\tau^{\mathbf{c}}(E) - \tau^{\mathbf{c}}(0)]/\tau^{\mathbf{c}}(0)$ based on the linear and conventional $U_N^c(X)$. Despite the anticipated singularity, the nonlinear $U_A(X)$ thus offers a marked improvement compared with the linear potentials commonly used for reflectrons, and the nonlinearity remains extremely small.

In conclusion, we described a simple inversion scheme, originated from AMP, for charged particles of the energies E to satisfy the perfect isochronicity of $\tau(E > 0) = \tau_0 =$ constant. Instead of the reflecting electric potential $U(X)$, its inverse function $X(U)$ is ideally determined by the Abel inversion of $\tau(E)$. To realize this inversion scheme, the major obstacle is a theoretical finding that $X(U \geq 0)$ always behaves singularly at the origin $X = U = 0$: $X(U \geq 0) =$ (analytic part) $- a_1 U^{3/2} - a_2 U^{5/2} - \cdots$. This feature is seemingly unfavorable for the electrostatic realization of $X(U)$. However, our theoretical and numerical analyses revealed that this singularity can be neatly controlled: we can set $a_1 = a_2 = \cdot\cdot = a_n = 0$ when $\frac{d\tau}{dE} = \frac{d^2\tau}{dE^2} = \cdot\cdot = \frac{d^n\tau}{dE^n} = 0$ at $E = 0$.

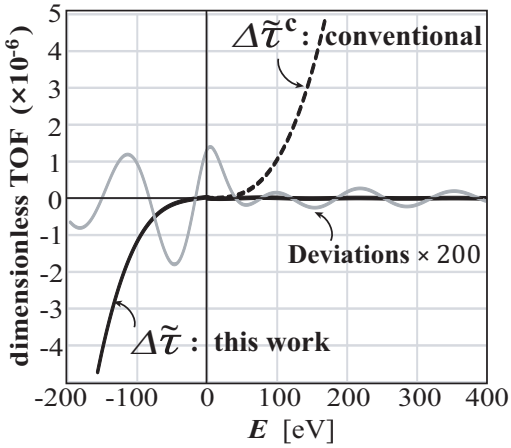

Fig. 4. Simulated TOF functions in dimensionless forms. $\Delta\tilde{\tau}$ [black solid] for the nonlinear $U_A(X)$ and $\Delta\tilde{\tau}^{\mathbf{c}}$ [dotted] for the linear and conventional $U_N^{\mathbf{c}}(X)$. The deviations of $\Delta\tilde{\tau}$ [gray solid] from the predetermined values are enlarged by 200.

Further challenges are on-going to identify and suppress the small but unfamiliar errors[10] still remaining for a reflectron improved using the present inversion scheme.

Acknowledgment

We are grateful to Shimadzu Corporation for the financial support providing during its collaboration with Kobe University. The authors would like to thank Enago (www.enago.jp) for the English language review.

References

1) N. H. Abel, J. Reine Angew. Mathematik **1**, 153 (1826).

2) R. Gorenflo and S. Vessella, *Abel Integral Equations - Analysis and Applications* p.1-2 (Springer, Berlin, 1991).

3) Kwan-ichi Terasawa, *Sizenkagakusya no tame no Sugaku Gairon* (Introduction to Mathematics for Natural Scientists) (Iwanami, Tokyo, 1981) p.580-582 [in Japanese].

4) L. D. Laudau and E. M. Lifshitz, *Mechanics* (Pergamon, Oxford, 1977) p.27-29.

5) We refer to the transformation from $\tau(E)$ to $X(U)$ as the Abel inversion although $X(U)$ is reversely related to the Abel transform of $\tau(E)$, as well.

6) T. Kinugawa, J. Math. Phys. **55**, 022903 (2014).

7) V. I. Karataev, B. A. Mamyrin and D. V. Shmikk, Sov. Phys.-Tech. Phys. **16**, 1177 (1972).

8) (Supplemental Material) Significant Suppression of the Turn-Around Time by Abel Inversion Scheme is provided online.

9) Similar spline interpolations are often used for the design of reflectrons after the instructive report by T. Bergmann, T. P. Martin and H. Schaber in Rev. Sci. instrum.**61**, 2592 (1990).

10) As detailed in Ref. 8, the turn-around time will be no longer crucial. So the authors believe that the most dominant error is caused by the off-axis aberration arising from the weak nonlinearity of $U_A(X)$, more specifically, the Y-dependence of $U_A(X,Y)$, as suggested by numerical simulations in the patented work: T. Kinugawa and O. Furuhashi, PCT Patent WO2012/086630 (2012).

Significant Suppression of the Turn-Around Time by Abel Inversion Scheme

Tohru Kinugawa[1], Osamu Furuhashi[2]

[1]*Institute for Promotion of Higher Education, Kobe University, Kobe 657-8501, Japan*
[2]*Technology Research Laboratory, Shimadzu Corporation, Kyoto 604-8511, Japan*

Although our letter focuses on the theoretical aspect of the Abel inversion scheme, the authors have been driven rather by a practical motivation: the significant suppression of the turn-around time.[1] As widely accepted in mass spectrometry, the turn-around time limits the maximum resolving power of any TOF spectrometer using a static potential $U(X)$. This supplemental material will help in understanding how the above goal of practical importance can be accomplished by the present inversion method while requiring nearly no familiarity with TOF mass spectrometry.

Let us begin by defining the turn-around time, based on Fig.1, which is a refinement of Fig.3 in Ref.1. This figure depicts the travel time T_{ta}, namely, the temporal interval that is spent by a charged particle produced in the source with the initial on-axis velocity V_i to reach the initial rest position. We also assume that the particle is initially accelerated (or decelerated, depending on the sign of V_i) by a uniform field F_s created around the start position. Formally we have

$$T_{ta} = -(M/q) \cdot V_i/F_s, \tag{1}$$

where M/q is the mass-to-charge ratio of the ion concerned. Next, we apply (1) to a pair of charged particles starting from the same position but initially released with the opposite on-axis velocities of $\pm|V_i|$. Since a static potential $U(X)$ is used in the spectrometer, these particles conserve the same energy E during their flights. As a result, they trace the identical parabolic trajectories in Fig.1, which are separated by the constant interval of $2T_{ta}$. In TOF mass spectrometry, this fixed shift of $2T_{ta}$ is called the turn-around time. Obviously, this turn-around time leads to the erroneous determination of M/q: for the above pair, their total TOFs T always differ by $2T_{ta}$ despite the same M/q. Since T_{ta} can not be 0 in (1) but can only be minimized, it is widely accepted that the turn-around time represents the minimum attainable width of TOF peaks.

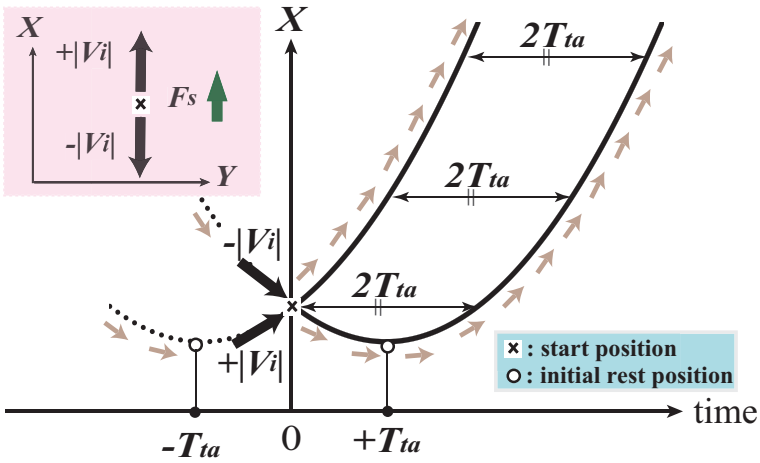

Fig. 1. Turn-around time $2T_{ta}$ for a pair of charged particles starting from the same position with the opposite on-axis velocities of $\pm|V_i|$.

For suppressing this turn-around time, we have only three solutions: (i) the maximization of the total TOF T for a constant T_{ta}, (ii) the minimization of $|V_i|$ and (iii) the maximization of $|F_s|$. Although the present inversion scheme is related to the solution (iii), let us first review (i) and (ii) that have been long established in TOF mass spectrometry.

The solution (i) is as simple as follows. From Eq. (1) in our letter, $T \propto \sqrt{M}$ and, therefore, the resolving power of a TOF mass spectrometer is given by

$$M/\Delta M = T/(2\Delta T), \tag{2}$$

where ΔM is the minimum resolvable mass difference around the mass M and ΔT is the broadening of the total TOF T, respectively. As a result, $M/\Delta M$ can be improved by maximizing T in (2) for a fixed ΔT. In short, the longer TOF spectrometer offers a better chance of improving the resolving power by reducing the relative influence of ΔT that reflects the turn-around time, as well. Apparently, this solution is a limited one because any real instrument cannot be infinitely long in its spatial size. Interestingly, this limitation is seemingly broken by those TOF spectrometers based on multi-reflection[2] and multi-turn.[3] These instruments enable the increase of the total TOF T, almost arbitrarily in principle, by increasing the repetitions of the linear reflections[2] or the circular turns[3] in the spectrometer. However, this increase is always accompanied by the serious degradation of the acceptable mass-window, due to the 'overtaking' problem.[4] Specifically, fast and light ions can overtake slow and heavy ones since all the ions repeat the periodic motion in the same closed orbit. Due to this overtaking, the number of repetitions and, thereby, M/q must remain undetermined by each TOF

peak, unless the time-gate is severely narrowed at the time of the ion injection into the periodic orbit.[4]

The second solution (ii) results directly from the above equation (1). There are two major methods established for reducing $|V_i|$ in practice. The first one is the orthogonal acceleration.[5] In this method, the ions are injected into a TOF spectrometer along a line orthogonal to the TOF axis so that the initial on-axis velocities are geometrically kept small. Second, $|V_i|$ can be further reduced by cooling the ions via collisions with some buffer gas[6] before the ions are injected into a TOF spectrometer.

Finally, we mention the solution (iii) that is also expected from (1) but has not been fully studied yet. In fact, this lack of comprehensive studies is attributed to the simple reason below: if $|F_s|$is increased, the ions inevitably gain the broader energy-spread $\Delta E \approx |F_s \times \Delta X|$ where ΔX is the width of the initial on-axis position. As a result, the TOF peaks are significantly broadened unless the total TOF T is independent of the energy E. From (2), this broadening readily leads to the degradation of the mas-resolving power. So there is a dilemma about the magnitude of F_s. If $|F_s|$is too large, $M/\Delta M$ can be degraded due to the dependence of T on the energy E. On the contrary, if $|F_s|$ is too small, this may lead to an excessive increase of the turn-around time. There is only one way to escape from this dilemma: making T completely independent of the energy E. The authors found that this ideal treatment is attainable only by the present inversion scheme. In conclusion, $|F_s|$ can be increased for the significant suppression of the turn-around time once the inversion scheme ensures the constant TOF T for a wide range of the energy E.

References

1) M. Guilhaus, *Principles and Instrumentation in Time-of-flightt Mass Spectrometry* J. Mass Spectrometry **30**, 1519 (1995).

2) H. Wollnik and A. Casares, *An energy-isochronous multi-pass time-of-flight mass spectrometer consisting of two coaxial electrostatic mirrors* Int. J. Mass Spectrom. **227**, 217 (2003).

3) M. Toyoda, D. Okumura, M. Ishihara and I. Katakuse, *Multi-turn time-of-flight mass spectrometers with electrostatic sectors* J. Mass Spectrom. **38**, 1125 (2003).

4) M. Nishiguchi, Y. Ueno, M. Toyoda and M. Setou, *Design of a new multi-turn ion optical system ' IRIS ' for a time-of-flight mass spectrometer* J. Mass Spectrom. **44**, 594 (2009).

5) M. Guilhaus, D. Selby and V. Mlynski, *ORTHOGONAL ACCELERATION TIME-OF-FLIGHT MASS SPECTROMETRY* Mass Spectrom. Rev. **19**, 65 (2000).

6) I. V. Chernushevich and B. A. Thomson, *Collisional cooling of large ions in electrospray mass spectrometry* Anal. Chem.**76**, 1754 (2004).